Dalton Transactions

Activation of the Manganese(I) Tricarbonyl Core by Selective Variation of Bidentate Ligands (L,L'-Bid = N,N'and N,O Donor Atom Sets) in fac-[Mn(CO)3(L,L'-Bid)(CH3OH)]n complexes.

Journal:	*Dalton Transactions*
Manuscript ID:	DT-ART-11-2014-003524.R1
Article Type:	Paper
Date Submitted by the Author:	23-Dec-2014
Complete List of Authors:	Twala, Thembani; University of the Free State, Department of Chemistry Schutte-Smith, Marietjie; Univeristy of the Free State, Department of Chemistry Roodt, Andreas; University of the Free State, Department of Chemistry Visser, Hendrik; University of the Free State, Department of Chemistry

Journal Name

RSCPublishing

ARTICLE

Activation of the Manganese(I) Tricarbonyl Core by Selective Variation of Bidentate Ligands (*L*,*L*'-Bid = *N*,*N*'and *N*,*O* Donor Atom Sets) in *fac*-$[Mn(CO)_3(L,L'\text{-Bid})(CH_3OH)]^n$ complexes.

Cite this: DOI: 10.1039/x0xx00000x

Received ooth January 2012,
Accepted ooth January 2012

DOI: 10.1039/x0xx00000x

www.rsc.org/

T. N. Twala, M. Schutte-Smith, A. Roodt, H.G. Visser*

A range of *fac*-$[Mn(CO)_3(L,L'\text{-Bid})(H_2O)]^n$ (*L*,*L*'-Bid = neutral or monoanionic bidentate ligands with varied *L*,*L*' donor atoms, *N*,*N*' and *N*,*O*, 1,10-phenanthroline, 2,2'-bipyridine, 2-picolinate, 2,4-quinolinate; n = 0, +1) has been synthesized and the methanol substitution has been investigated for the first time. The complexes were characterized by UV/vis, IR and NMR spectroscopy and X-ray crystallographic studies of the compounds *fac*-$[Mn(CO)_3(Bipy)(H_2O)][CF_3SO_3]$ (**1**) and *fac*-$[Mn(CO)_3(Phen)(H_2O)][CF_3SO_3]$ (**6**) are reported. A two order-of-magnitude of activation for the methanol substitution is induced as manifested by the second order rate constants with (*N*,*N*'-Bid) < (*N*,*O*-Bid). Forward and reverse rate and stability constants from slow and stopped-flow UV/vis measurements (k_1, M^{-1} s^{-1}; k_{-1}, s^{-1}; K_1, M^{-1}) for pyridine as entering nucleophile are as follows: *fac*-$[Mn(CO)_3(Phen)(CH_3OH)]^+$ $(2.39 \pm 5) \times 10^{-3}$, $(1.5 \pm 0.3) \times 10^{-5}$, 159 ± 32; *fac*-$[Mn(CO)_3(2,4\text{-QuinH})(CH_3OH)]$ (4.5 ± 0.2), $(4 \pm 1) \times 10^{-2}$, 113 ± 29. Activation parameters ($\Delta H_{k1}^{\neq}$, kJ mol^{-1}; $\Delta S_{k1}^{\neq}$, J K^{-1} mol^{-1}) from Eyring plots for entering nucleophiles as indicated are as follows: *fac*-$[Mn(CO)_3(Phen)(CH_3OH)]^+$ (bromide ions) 66.7 ± 0.6, −27 ± 2; (pyridine) 80 ± 3, −25 ± 11; *fac*-$[Mn(CO)_3(Pico)(CH_3OH)]$ (bromide ions) 68 ± 2, −24 ± 5. A dissociative interchange mechanism is proposed.

Introduction

Low-oxidation state aqua carbonyl complexes of group 7 elements (Mn, Tc, Re) have gained much attention because of the high stability of the *fac*-$\{M(CO)_3\}$ core and possible applications as radiopharmaceuticals in the case of ^{99m}Tc and $^{186/188}$Re. The main reason for the interest in these complexes in terms of radiopharmacy lies in the versatility when synthesizing new complexes. The stable *fac*-$\{M(CO)_3\}$ fragment reacts readily with various bidentate and tridentate chelators to form very stable complexes, hence it is no wonder that several promising compounds linked to bio-molecules were introduced in the last few years.[1,2,3,4,5,6,7,8,9,10,11]

In order to develop new methods for the production of radiolabeled compounds in a therapeutic or diagnostic environment, kinetic studies are required to give insights into reactivity, stability and the mechanism of complex formation. The synthesis of radiolabeled compounds is a very time specific process since the half-life of the radionuclide and other factors like solubility and purity of the final prepared species all play a role in the success of said compound. The bottom-line in the case of the *fac*-$\{M(CO)_3\}$ core is that three water molecules have to be substituted and that the upper limit of the time aspect is the rate of water self-exchange in the complex itself. An interesting aspect of radiopharmaceutical design in this field involves the so-called [2 + 1] approach which involves different choices of bidentate ligands as chelators and biologically active directing ligands in the third position or variations on this where the directing ligand is attached to the chelating bidentate.[14]

There are several very interesting studies that investigated the kinetics of the aqua carbonyl complexes of the group 7 elements. Salignac and co-workers provided the first thermodynamic and kinetic data for water exchange on *fac*-$[Re(CO)_3(H_2O)_3]^+$ through NMR techniques[12] and the data for the Tc(I) and Mn(I) counterparts was published shortly thereafter.[13] The entropy of activation values and the fact that the rate of water exchange was similar to the rate of water substitution by a variety of entering ligands indicated a

dissociatively activated process. It was also shown that the water exchange depends strongly on the metal center, with $k_{ex}(Mn) > k_{ex}(Tc) > k_{ex}(Re)$.

The fact that the *fac*-{$Re(CO)_3$} core produced slower rates of exchange than the comparative Tc(I) complexes, does not exclude it from potential use as a radionuclide in radiopharmacy, in fact, a few papers suggest otherwise.[4,5,6,7,8,9,10] It was shown that the choice of bidentate ligand, following the [2 + 1] approach first introduced by Mundwiler *et al.*,[14] could tune the rate of substitution of the coordinated solvent species , in *fac*-[$Re(CO)_3$(*L,L'*-Bid)(CH_3OH)] (*L,L'*-Bid = neutral or monoanionic bidentate ligands), in this case methanol, in the third position, by four orders-of-magnitude.[15] The most significant activation of the rhenium center was achieved with *O,O'* bidentate ligand systems. Later on, it was shown that the rate of substitution of a coordinated water ligand is about 10 times faster than for coordinated methanol in *fac*-[$Re(CO)_3$(Trop)(S)] (S = CH_3OH or H_2O and $Trop^-$ = tropolonate).[16] Both these mentioned studies indicated a dissociative activation for substitution in these reactions.

Interestingly, the substitution reactions of coordinated methanol in a range of different *fac*-[$Re(CO)_3$(*L,L'*-Bid)(CH_3OH)] (*L,L'*-Bid = salicylidene bidentate ligand systems), yielded non-linear kinetic plots in some cases.[17] These results pointed to an I_d mechanism. The second order rate constants (k_1) for these reactions were considerably larger than what was found earlier for other N,O bidentate ligand systems, indicating higher activation of the metal center when the Schiff base ligands are employed.

The aqueous kinetics of *fac*-$[Mn(CO)_3]^+$ complexes is virtually unexplored. This, together with the fact that previous work have shown that the rate of substitution reactions of Mn(I) > Tc(I) > Re(I) and that the corresponding work on *fac*-[$Re(CO)_3$(*L,L'*-Bid)(CH_3OH)] indicated a 20 000 times increase in rate depending on the bidentate ligand used, provides invaluable evidence for future radiopharmaceutical design. Not only can the kinetic study provide an upper limit of reactivity (when moving down in the series from Mn to Re), but Mn(I) like Re(I) is an excellent model for the Tc(I) counterpart. To achieve this and in order to make a reasonable comparison with the published work on Re(I), it was decided to study the methanol substitution by various monodentate ligands in *fac*-[$Mn(CO)_3$(*L,L'*-Bid)(CH_3OH)]^n (*L,L'*-Bid = neutral or monoanionic bidentate ligands with varied *L,L'* donor atoms, *N,N'* or *N,O'*: 1,10-phenanthroline (Phen), 2,2'-bipyridine (Bipy), 2-picolinate (PicoH) and quinoline-2-carboxylate-4-carboxylic acid (2,4-$QuinH_2$), n = 0, +1).

Two crystal structures, *fac*-[$Mn(CO)_3$(Phen)(H_2O)][CF_3SO_3] and *fac*-[$Mn(CO)_3$(Bipy)(H_2O)][CF_3SO_3] are also reported (together with NMR, IR, UV/vis) to fully characterise starting complexes and products and expand the knowledge base of these systems. A search of the Cambridge Structural Database (CSD) revealed only two other [2 + 1] structures with a coordinated water ligand in the third position.[18]

Experimental

The reagents used for synthesis and characterization were purchased from Sigma-Aldrich, South Africa, unless stated otherwise and were used as purchased. Quinoline-2,4-dicarboxylic acid was purchased from Merck, South Africa, and methanol-d^4 and acetone-d^6 were purchased from Cambridge Isotope Laboratories, Inc. All UV-vis measurements were collected using a Varian Cary 50 Conc UV-Visible spectrophotometer, equipped with a Julabo F12-mV temperature cell regulator (accurate within 0.1 °C) in a 1.000 ± 0.001 cm quartz cuvette cell.

The more rapid reactions ($t_{1/2}$ < 20 s) were first evaluated on a third generation Hi Tech SF61DX2 Stopped Flow System equipped with a diode array (dead time < 5 ms; 400 nm spectral width scans collected at < 5 ms/complete scan), with a thermostatted SHU61DX sample handling unit and an attached Julabu MPV thermostatted water bath (accurate within 0.05 °C) to select the best absorbance difference regions for the most accurate monitoring of the reactions. This was then followed on the stopped-flow in photo-multiplier mode (dead time *ca.* 1 ms) to monitor the actual reactions. The values reported (see supporting information) consist of the average of 5 individual traces per concentration.

The NMR spectra were obtained on a Bruker Avance II 600 MHz and a Bruker DVX 300 MHz spectrometer. The chemical shifts are reported in ppm relative to TMS (^1H and ^{13}C) using methanol-d^4 (3.31 ppm and 4.71 ppm, 49.15 ppm), acetone-d^6 (2.05 ppm, 29.92 ppm and 206.68 ppm) and DMSO-d^6 (2.54 ppm, 40.45 ppm). All infrared spectra were recorded on a Bruker Tensor 27 Standard System spectrophotometer with a laser range of 4000 – 370 cm^{-1}.

All synthetic procedures were performed in the dark while all the N,O-bidentate complexes were synthesized under nitrogen gas. The long relaxation times of specifically carbonyl ligands, together with the low solubility of most of these complexes result in many of these complexes not being observed on ^{13}C NMR, however the presence of the carbonyl ligands are clearly detected on the IR spectra. Scheme 1 presents the synthesized complexes.

Scheme 1. Representation of the complexes synthesized.

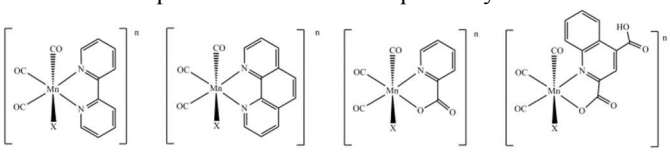

***fac*-[$Mn(CO)_3$(Bipy)(H_2O)][CF_3SO_3] (1).**

$Mn(CO)_5Br$ (0.2751 g, 1.0 x 10^{-3} mol) was dissolved in 20 mL acetone. $AgCF_3SO_3$ (0.771 g, 3.0 x 10^{-3} mol) dissolved in 20 mL acetone was added to the mixture and stirred for 45 hours at room temperature. A precipitate (AgBr) formed; it was filtered off and weighed (0.563 g, 3.0 x 10^{-3} mol). The yellow solution was dried under vacuum and a yellow oil formed. 2,2'-

Bipyridyl (0.1760 g, 1.1 x 10^{-3} mol) was suspended in 10 mL water and was added to the yellow oil and the reaction was refluxed for 24 hours at 110 °C. The dark orange solution was then cooled to room temperature and left to crystallise. Orange-red cuboidal crystals, suitable for X-ray diffraction were obtained. Yield = 0.105 g; 22.7 %. UV/vis: λ_{max} = 395 nm, ε = 1460 M^{-1} cm^{-1}. IR (KBr, cm^{-1}): υ_{CO} = 1933, 2040. ^{1}H NMR (Acetone-d^6): δ = 9.45 (dd, 2H, J = 16.1Hz, 5.4Hz), 8.76 (dd, 2H, J = 8.1 Hz, 1.2 Hz), 8.46 (tt, 2H, J = 8.2 Hz, 5.1 Hz), 7.93 (tt, 2H, J = 8.2 Hz, 5.1 Hz). ^{13}C NMR (Acetone-d^6): δ = 125.05, 129.15, 142.22, 155.90, 157.91. Anal. Calcd: C, 36.38; H, 2.18; N, 6.06. Anal. Found: C, 36.78; H, 2.11; N, 6.12. ***fac*-[Mn(CO)$_3$(Bipy)(CH$_3$OH)][CF$_3$SO$_3$] (2).** *fac*-[Mn(CO)$_3$(Bipy)H$_2$O][CF$_3$SO$_3$] (0.030 g, 6.490 x 10^{-5} mol) was dissolved in methanol (10 mL) and the solution was stirred overnight at room temperature. The solution was dried and a yellow precipitate was collected. Yield = 0.0288 g, 93.2 %. UV/vis: λ_{max} = 402 nm, ε = 1276 M^{-1} cm^{-1}. IR (KBr, cm^{-1}): υ_{CO} = 1941, 2038. ^{1}H NMR (Acetone-d^6): δ = 9.75 (dd, 2H, *J* = 16.1Hz, 5.4Hz), 8.99 (dd, 2H, *J* = 8.1 Hz, 1.2 Hz), 8.35 (tt, 2H, *J* = 8.2 Hz, 5.1 Hz), 8.23 (tt, 2H, *J* = 8.2 Hz, 5.1 Hz), 3.78 (s, 3H). ^{13}C NMR (Acetone-d^6): δ = 126.43, 127.63, 130.26, 139.51, 155.03. Anal. Calcd: C, 37.83; H, 2.54; N, 5.88. Anal. Found: C, 37.90; H, 2.61; N, 6.00. ***fac*-[Mn(CO)$_3$(Bipy)(Br)] (3).** *fac*-[Mn(CO)$_3$(Bipy)H$_2$O][CF$_3$SO$_3$] (0.030 g, 6.490 x 10^{-5} mol) was dissolved in methanol after which an equimolar amount of NaBr in methanol (20 mL) was added. The solution was stirred overnight at room temperature and left to stand until an orange precipitate formed. Yield = 0.0227 g, 93.3 %. UV/vis: λ_{max} = 416 nm, ε = 938 M^{-1} cm^{-1}. IR (KBr, cm^{-1}): υ_{CO} = 1894, 2025. ^{1}H NMR Acetone-d^6): δ = 9.65 (dd, 2H, *J* = 8.0 Hz, 1.1 Hz), 8.83 (dd, 2H, *J* = 8.1 Hz, 1.2 Hz), 8.26 (tt, 2H, *J* = 5.1 Hz, 8.2 Hz), 8.11 (tt, 2H, *J* = 5.1 Hz, 8.2 Hz). ^{13}C NMR (Acetone-d^6): δ = 125.62, 127.24, 130.26, 137.75, 154.25. Anal. Calcd: C, 41.63; H, 2.15; N, 7.47. Anal. Found: C, 41.75; H, 2.19; N, 7.58. ***fac*-[Mn(CO)$_3$(Bipy)(Py)][CF$_3$SO$_3$] (4).** *fac*-[Mn(CO)$_3$(Bipy)(H$_2$O)][CF$_3$SO$_3$] (0.030 g, 6.490 x 10^{-5} mol) was dissolved in methanol after which an excess of pyridine was added and the solution was stirred overnight at room temperature. The solution was left to stand until an orange yellow precipitate formed. Yield = 0.0312 g, 91.9 %. UV/vis: λ_{max} = 388 nm, ε = 1262 M^{-1} cm^{-1}. IR (KBr, cm^{-1}): υ_{CO} = 2023, 1924. ^{1}H NMR (Acetone-d^6): δ = 10.02 (dd, 2H, *J* = 5.1 Hz, 1.2 Hz), 9.02 (dd, 2H, *J* = 8.1 Hz, 1.2 Hz), 8.58 (tt, 2H, *J* = 6.5 Hz, 8.2 Hz), 8.35 (tt, 2H, *J* = 8.2 Hz, 5.1 Hz), 8.32 (t, 1H, J = 9.6 Hz), 7.83 (tt, 2H, *J* = 7.6 Hz, 1.5 Hz), 7.33 (tt, 2H, *J* = 7.5 Hz, 6.6 Hz). ^{13}C NMR (Acetone-d^6): δ = 126.17, 127.09, 127.78, 130.51, 139.46, 146.33, 152.57, 155.23. Anal. Calcd: C, 43.61; H, 2.50; N, 8.03. Anal. Found: C, 43.74; H, 2.53; N, 7.95. ***fac*-[Mn(CO)$_3$(Bipy)(TU)][CF$_3$SO$_3$] (5).** *fac*-[Mn(CO)$_3$(Bipy)H$_2$O][CF$_3$SO$_3$] (0.030 g, 6.490 x 10^{-5} mol) was dissolved in a 0.2 M solution of thiourea (excess) in methanol and the solution was stirred overnight at room temperature. The solution was dried and a yellow precipitate was collected after several days. Yield = 0.0304 g, 90.0 %. UV/vis: λ_{max} = 400 nm, ε = 924 M^{-1} cm^{-1}. IR (KBr, cm^{-1}): υ_{CO} = 2030, 1925. ^{1}H NMR (Acetone-d^6): δ = 9.65 (dd, 2H, *J* = 5.0 Hz, 1.0 Hz), 8.94 (dd, 2H, *J* = 27.3 Hz, 13.6 Hz), 8.35 (tt, 2H, *J* = 6 Hz, 7.2 Hz), 8.20 (tt, 2H, *J* = 21.7 Hz, 10.9 Hz), 6.91 (s, 4H). ^{13}C NMR (Acetone-d^6): δ = 126.34, 127.61, 130.56, 138.49, 146.21, 154.12, 181.04, 185.55. Anal. Calcd: C, 34.62; H, 2.32; N, 10.77. Anal. Found: C, 34.75; H, 2.41; N, 10.85. ***fac*-[Mn(CO)$_3$(Phen)(H$_2$O)][CF$_3$SO$_3$] (6).** Mn(CO)$_5$Br (0.2751 g, 1.0 x 10^{-3} mol) was dissolved in 20 mL acetone. $AgCF_3SO_3$ (0.771 g, 3.0 x 10^{-3} mol) dissolved in 20 mL acetone was added to the mixture and stirred for 45 hours at room temperature. A yellow solution with a grey precipitate formed. AgBr was filtered off and the precipitate was weighed (0.563 g, 3.0 x 10^{-3} mol). The filtrate was dried under vacuum and a yellow oil formed. 1,10'-Phenanthroline (0.1810 g, 1.0 x 10^{-3} mol) was suspended in 10 mL water and added to the yellow oil and the reaction mixture was refluxed for 24 hours at 110 °C. The dark orange solution was then cooled down to room temperature and left to stand to form crystals. Orange needle-like crystals, suitable for X-ray diffraction were obtained. Yield = 0.1256 g, 25.8 %. UV/vis: λ_{max} = 400 nm, ε = 1148 M^{-1} cm^{-1}. IR (KBr, cm^{-1}): υ_{CO} = 2041, 1940. ^{1}H NMR (Acetone-d^6): δ = 9.70 (dd, 2H, *J* = 5.1 Hz, 1.3Hz), 8.91 (dd, 2H, *J* = 8.3 Hz,1.3 Hz), 8.26 (d, 2H, *J* = 4.7 Hz), 8.15 (dd, 2H, *J* = *8*.3 Hz, 5.1 Hz). ^{13}C NMR (Acetone-d^6): δ = 126.04, 127.34, 130.40, 139.21, 146.77, 154.44. Anal. Calcd: C, 39.52; H, 2.07; N, 5.76. Anal. Found: C, 39.75; H, 2.09; N, 5.84. ***fac*-[Mn(CO)$_3$(Phen)(CH$_3$OH)][CF$_3$SO$_3$] (7).** *fac*-[Mn(CO)$_3$(Phen)(H$_2$O)][CF$_3$SO$_3$] (0.030 g, 6.170 x 10^{-5} mol) was dissolved in methanol (10 mL of a 0.5 × 10^{-3} M solution) and the solution was stirred overnight at room temperature. The solution was dried to give a yellow-orange precipitate. Yield = 0.0288 g, 93.3 %. UV/vis: λ_{max} = 405 nm, ε = 2000 M^{-1} cm^{-1}. IR (KBr, cm^{-1}): υ_{CO} = 2025,1894. ^{1}H NMR (Acetone-d^6): δ = 9.80 (dd, 2 H,*J* = 2.8 Hz,2.1Hz), 9.03 (dd, 2H, *J* = 8.2 Hz,1.3 Hz), 8.39 (d, 2H, *J* = 7.1 Hz), 8.27 (dd, 2H, *J* = *8*.2 Hz, 5.1 Hz), 3.80 (s, 3H). ^{13}C NMR (Acetone-d^6): δ = 126.43, 127.59, 130.31, 139.47, 147.43, 155.03. Anal. Calcd: C, 40.81; H, 2.42; N, 5.60. Anal. Found: C, 40.89; H, 2.49; N, 5.70. ***fac*-[Mn(CO)$_3$(Phen)(Br)] (8).** *fac*-[Mn(CO)$_3$(Phen)(H$_2$O)][CF$_3$SO$_3$] (0.030 g, 6.170 x 10^{-5} mol) was dissolved in a 0.2 M solution of NaBr (excess) in methanol and stirred overnight at room temperature. An orange precipitate formed after one day. Yield = 0.0226 g, 91.8 %. UV/vis: λ_{max} = 413 nm, ε = 1254 M^{-1} cm^{-1}. IR (KBr, cm^{-1}): υ_{CO} = 2017, 1907. ^{1}H NMR (Acetone-d^6): δ = 9.67 (dd, 2H, *J* = 4.0 Hz), 8.85 (dd, 2H, *J* = 7.1Hz), 8.28 (dd, 2H, J = 8.2 Hz, 5.1 Hz), 8.13 (dd, 2H, *J* = *8*.1 Hz, 5.1 Hz). ^{13}C NMR (Acetone-d^6): δ = 125.44, 126.38, 130.77, 141.41, 148.23, 155.47. Anal. Calcd: C, 45.15; H, 2.02; N, 7.02. Anal. Found: C, 45.24; H, 2.17; N, 7.13. ***fac*-[Mn(CO)$_3$(Phen)(Py)][CF$_3$SO$_3$] (9).** *fac*-[Mn(CO)$_3$(Phen)(H$_2$O)][CF$_3$SO$_3$] (0.030 g, 6.170 x 10^{-5} mol) was dissolved in methanol after which a few drops of pyridine was added (excess). A yellow precipitate formed after stirring overnight at room temperature. Yield = 0.0314 g, 93.0 %. UV/vis: λ_{max} = 375 nm, ε = 1466 M^{-1} cm^{-1}. IR (KBr, cm^{-1}):

υ_{CO} = 2025, 1932. ^{1}H NMR (Acetone-d^6): δ = 10.05 (dd, 2 H), 9.06 (dd, 2H, *J* = 6.5 Hz), 8.59 (d, 2H, *J* = 24.3 Hz), 8.31 (dd, 2H, *J* = 46.5 Hz), 8.61 (d, 2H, *J* = 24.3 Hz), 7.80 (d, 1H, *J* = 37.8 Hz), 7.35 (s, 2H). ^{13}C NMR (Acetone-d^6): δ = 126.21, 127.26, 127.78, 127.93, 139.51, 145.56, 145.69, 152.72, 155.35. Anal. Calcd: C, 46.08; H, 2.39; N, 7.68. Anal. Found: C, 46.21; H, 2.46; N, 7.76. ***fac*-[Mn(CO)$_3$(Phen)(TU)][CF$_3$SO$_3$] (10).** *fac*-[Mn(CO)$_3$(Phen)(H$_2$O)][CF$_3$SO$_3$] (0.030 g, 6.170 x 10^{-5} mol) was dissolved in a 0.2 M solution of thiourea (excess) in methanol and the solution was stirred overnight at room temperature. A yellow precipitate formed after two days. Yield = 0.0303 g, 83.9 %. UV/vis: λ_{max} = 403 nm, ε = 1520 M^{-1} cm^{-1}. IR (KBr, cm^{-1}): υ_{CO} = 2030, 1940, 1920. ^{1}H NMR (Acetone-d^6): δ = 9.63 (dd, 2 H, *J* = 17.6 Hz), 8.93 (dd, 2H, *J* = 25.1 Hz), 8.33 (d, 2H, *J* = 29.8 Hz), 8.19 (dd, 2H, *J* = 57.8 Hz, 28.9 Hz), 6.92 (s, 4H). ^{13}C NMR (Acetone-d^6): δ = 126.34, 127.61, 130.26, 138.49, 146.20, 154.12, 185.59. Anal. Calcd: C, 37.51; H, 2.22; N, 11.76. Anal. Found: C, 37.58; H, 2.29; N, 11.66. ***fac*-[Mn(CO)$_3$(Pico)(H$_2$O)] (11).** Mn(CO)$_5$Br (0.2741 g, 0.997 mmol) was dissolved in 20 mL acetone. $AgCF_3SO_3$ (0.3112 g, 1.2 mmol) dissolved in 20 mL acetone was added to the mixture and refluxed at 60°C for 1 hour. The precipitate (AgBr) was filtered off and weighed (0.0467 g, 0.25 mmol). The yellow solution was then dried under vacuum to form a yellow oil. Picolinic acid (0.1230 g, 0.995 mmol) dissolved in 10 mL water was added to the yellow oil and refluxed at 110°C for 24 hours under nitrogen. The bright yellow solution was dried under vacuum to form a yellow precipitate. Yield: 0.0986g, 35.4 %. UV/vis: λ_{max} = 385 nm, ε = 1666 M^{-1} cm^{-1}. IR (KBr, cm^{-1}): υ_{CO} = 2034, 1934, 1912. ^{1}H NMR (Acetone-d^6): δ = 9.21(d, 1H, *J* = 8.2 Hz), 8.60 (d, 1H, *J* = 8.2 Hz), 8.02 (t, 1H, *J* = 9.6 Hz), 7.50 (t, 1H, *J* = 9.6 Hz). ^{13}C NMR (Acetone-d^6): δ = 119.23, 121.83, 125.64, 128.14, 139.93, 152.70, 208.70, 209.08. Anal. Calcd: C, 38.46 (38.73); H, 2.87 (2.17); N, 4.98 (5.02). Anal. Found: C, 38.55; H, 2.93; N, 5.05. ***fac*-[Mn(CO)$_3$(Pico)(CH$_3$OH)] (12).** *fac*-[Mn(CO)$_3$(Pico)(H$_2$O)] (0.0225 g, 8.062 x 10^{-5} mol) was dissolved in methanol and the solution was stirred overnight at room temperature. The solution was dried and a yellow-orange precipitate was the result. Yield = 0.0214 g, 90.6 %. UV/vis: λ_{max} = 387 nm, ε = 3675 M^{-1} cm^{-1}. IR (KBr, cm^{-1}): υ_{CO} = 2028, 1931, 1907. ^{1}H NMR (Acetone-d^6): δ = 9.28 (d, 1H, *J* = 8.4 Hz), 8.66 (d, 1H, *J* = 8.4 Hz), 8.11 (t, 1H, *J* = 9.5 Hz), 7.77 (t, 1H, *J* = 9.5 Hz), 3.81 (s, 3H). ^{13}C NMR (Acetone-d^6): δ = 131.20, 125.75, 126.01, 129.88, 141.11, 153.01. Anal. Calcd: C, 40.70 (40.98); H, 3.42 (2.75); N, 4.75(4.78). Anal. Found: C, 40.78; H, 3.31; N, 4.87. ***fac*-[Mn(CO)$_3$(Pico)(TU)] (13).** *fac*-[Mn(CO)$_3$(Pico)(H$_2$O)] (0.0225 g, 8.062 x 10^{-5} mol) was dissolved in a 0.2 M solution of thiourea (excess) in methanol and the solution was stirred overnight at room temperature. An orange yellow precipitate formed after one day. Yield = 0.0247 g, 90.9 %. UV/vis: λ_{max} = 385 nm, ε = 1785 M^{-1} cm^{-1}. IR (KBr, cm^{-1}): υ_{CO} = 2025, 1928, 1901. ^{1}H NMR (Acetone-d^6): δ = 9.08 (d, 1H, *J* = 8.1 Hz), 8.44 (d, 1H, *J* = 8.1 Hz), 8.09 (t, 1H, *J* = 9.2 Hz), 7.91 (t, 1H, *J* = 9.3 Hz), 7.18 (s, 4H). ^{13}C NMR (Acetone-d^6): δ = 130.88, 124.90, 125.81, 130.05, 140.71, 152.87, 185.04. Anal. Calcd: C, 35.62; H, 2.98 (2.39); N, 12.46. Anal. Found: C, 35.71; H, 3.10; N, 12.51. ***fac*-[Mn(CO)$_3$(Pico)(Br)][Na] (14).** *fac*-[Mn(CO)$_3$(Pico)(H$_2$O)] (0.0225 g, 8.062 x 10^{-5} mol) was dissolved in a 0.2 M solution of NaBr in methanol and the solution was stirred overnight at room temperature. An orange precipitate formed after slow evaporation. Yield = 0.0253 g, 86.2 %. UV/vis: λ_{max} = 415 nm, ε = 1680 M^{-1} cm^{-1}. IR (KBr, cm^{-1}): υ_{CO} = 2030, 1930, 1909. ^{1}H NMR (Acetone-d^6): δ = 9.11 (d, 1H, *J* = 8.4 Hz), 8.53 (d, 1H, *J* = 8.4 Hz), 8.00 (t, 1H, *J* = 9.5 Hz), 7.82 (t, 1H, *J* = 9.5 Hz). ^{13}C NMR (Acetone-d^6): δ = 130.88, 124.90, 125.81, 130.05, 140.71, 152.87, 185.04. 130.78, 126.05, 126.09, 128.97, 140.89, 154.21. Anal. Calcd: C, 29.70; H, 1.11; N, 3.85. Anal. Found: C, 29.73; H, 1.10; N, 3.89. ***fac*-[Mn(CO)$_3$(Pico)(Py)] (15).** *fac*-[Mn(CO)$_3$(Pico)(H$_2$O)] (0.0225 g, 8.062 x 10^{-5} mol) was dissolved in a few drops of pyridine and the solution was stirred overnight at room temperature. An orange yellow precipitate formed after slow evaporation. Yield = 0.0250 g, 91.2 %. UV/vis: λ_{max} = 365 nm, ε = 1680 M^{-1} cm^{-1}. IR (KBr, cm^{-1}): υ_{CO} = 2023, 1929, 1903. ^{1}H NMR (Acetone-d^6): δ = 9.22 (d, 1H, *J* = 8.2 Hz), 8.61 (d, 2H, *J* = 6.3 Hz), 8.48 (d, 1H, *J* = 8.1 Hz), 8.04 (t, 1H, *J* = 9.6 Hz), 7.75 (t, 1H, *J* = 9.6 Hz), 7.59 (dt, 1H, *J* = 6.3 Hz, 3.1 Hz), 7.48 (s, 2H). ^{13}C NMR (Acetone-d^6): δ = 131.20, 125.75, 126.01, 126.54, 129.88, 138.56, 141.11, 145.21, 153.01. Anal. Calcd: C, 49.43; H, 2.67; N, 8.24. Anal. Found: C, 49.53; H, 2.71; N, 8.26. ***fac*-[Mn(CO)$_3$(2,4-QuinH)(H$_2$O)] (16).** Mn(CO)$_5$Br (0.2740 g, 0.997 mmol) was dissolved in 20 mL acetone. A solution of $AgCF_3SO_3$ (0.3111 g, 1.2 mmol) dissolved in 20 mL acetone was added to the mixture and refluxed at 60 °C for 1 hour. The precipitate (AgBr) was filtered off and the yellow solution was then dried under vacuum to form a yellow oil. Quinoline-2,4-dicarboxylic acid (0.2175 g, 1 mmol) dissolved in 10 mL water was added to the oil and refluxed at 110 °C for 24 hours under nitrogen. An orange-red precipitate was formed after slow evaporation. Yield: 0.1130g, 30.4%. UV/vis: λ_{max} = 392 nm, ε = 2405 M^{-1} cm^{-1}. IR (KBr, cm^{-1}): υ_{CO} = 2034, 1940, 1903. ^{1}H NMR (Acetone-d^6): δ = 9.13 (d, 1H, *J* = 8.7Hz), 8.97 (d, 1H, *J* = 8.6 Hz), 8.25 (t, 1H, *J* = 18 Hz), 8.01 (t, 1H, *J* = 18 Hz), 7.45 (s,1H).). ^{13}C NMR (Acetone-d^6): δ = 121.81, 126.84, 128.45, 130.58, 132.15, 139.15, 148.83, 151.62, 175.00. Anal. Calcd: C, 45.06; H, 2.16; N, 3.75. Anal. Found: C, 45.12; H, 2.20; N, 3.77. ***fac*-[Mn(CO)$_3$(2,4-QuinH)(CH$_3$OH)] (17).** *fac*-[Mn(CO)$_3$(2,4-QuinH)(H$_2$O)] (0.030 g, 8.040 x 10^{-5} mol) was dissolved in methanol, stirred overnight at room temperature and dried *in vacuo*. A dark orange precipitate was obtained from this. Yield = 0.0281 g, 90.3 %. UV/vis: λ_{max} = 398 nm, ε = 1792 M^{-1} cm^{-1}. IR (KBr, cm^{-1}): υ_{CO} = 2037, 1907. ^{1}H NMR (Acetone-d^6): δ = 9.20 (d, 1H, *J* = 8.6Hz), 8.87 (d, 1H, *J* = 8.6 Hz), 8.25 (t, 1H, *J* = 18.2 Hz), 8.13 (t, 1H, *J* = 18.2 Hz), 7.52 (s, 1H), 3.81 (s, 3H). ^{13}C NMR (Acetone-d^6): δ = 123.86, 125.85, 130.65, 131.53, 132.89, 140.26, 149.03, 152.55, 178.02. Anal. Calcd: C, 46.53; H, 2.60; N, 3.62. Anal. Found: C, 46.56; H, 2.71; N, 3.65. ***fac*-[Mn(CO)$_3$(2,4-QuinH)(TU)] (18).** *fac*-

$[Mn(CO)_3(2,4\text{-QuinH})(H_2O)]$ was dissolved in a 0.2 M solution of thiourea (excess) in methanol and the solution was stirred overnight at room temperature. An orange precipitate formed upon slow evaporation of the solvent. Yield = 0.0297 g, 85.7 %. UV/vis: λ_{max} = 395 nm, ε = 1252 M^{-1} cm^{-1}. IR (KBr, cm^{-1}): υ_{CO} = 2027, 1910. ^{1}H NMR (Acetone-d^6): δ = 8.90 (d, 1H, J = 8.6Hz), 8.53 (d, 1H, J = 8.6Hz), 8.05 (t, 1H, J = 18.2 Hz), 7.91 (s, 1H), 7.61 (t, 1H, J = 18.2 Hz), 7.15 (s, 4H). ^{13}C NMR (Acetone-d^6): δ = 121.31, 127.08, 127.70, 129.73, 131.56, 149.15, 153.02, 181.86, 183.97. Anal. Calcd: C, 43.35 (41.78); H, 2.27 (2.34); N, 9.48 (9.74). Anal. Found: C, 43.41; H, 2.26; N, 9.57. ***fac*-[Mn(CO)$_3$(2,4-QuinH)(Py)] (19).** *fac*-$[Mn(CO)_3(2,4\text{-QuinH})(H_2O)]$ (0.0225 g, 8.062 x 10^{-5} mol) was dissolved in methanol (20 mL) and a few drops of pyridine (excess) was added. The solution was stirred overnight at room temperature and allowed to stand. A precipitate formed after two days. Yield = 0.0323 g, 92.5 %. UV/vis: λ_{max} = 380 nm, ε = 1480 M^{-1} cm^{-1}. IR (KBr, cm^{-1}): υ_{CO} = 2024, 1906. ^{1}H NMR (Acetone-d^6): δ = 9.23 (d, 1H, J = 8.6Hz), 9.02 (d,1H, J = 8.6Hz), 8.96 (t, 1H, J = 25.1 Hz), 8.60 (t, 1H, J = 9.7 Hz), 8.25 (s, 1H), 8.12 (m, 2H), 8.01(t, 2H, J = 9.6 Hz), 7.66 (s, 2H). ^{13}C NMR (Acetone-d^6): δ = 123.90, 126.88, 127.82, 130.55, 131.60, 132.65, 139.55, 145.42, 145.49, 148.83, 153.68, 176.44. Anal. Calcd: C, 52.55; H, 2.55; N, 6.45. Anal. Found: C, 52.59; H, 2.54; N, 6.53.

X-ray Structure Determinations

Diffraction data for **1** and **6** was obtained by using a Bruker X8 Apex II 4K diffractometer. The apparatus was equipped with graphite monochromated Mo Kα radiation, with a wavelength of 0.71073 Å and with ω- and φ-scans at 100 K. The cell refinement was performed with SAINT-Plus[19] and the data reduction with SAINT-Plus and XPREP19. The absorption corrections were obtained by the use of the multi-scan technique and SADABS[20] software package. The two structures were solved using the SIR-97[21] package and refined with SHELXL-97[22] and WinGX.[23] The molecular graphics were done with DIAMOND.[24] All the structures are shown with thermal ellipsoids drawn at 50% probability level, unless otherwise stated. The aromatic hydrogen atoms are geometrically placed in idealized positions (C-H = 0.93 Å) and constrained to ride on their parent atoms (U_{iso} (H) = 1.2U_{eq}(C)). Aqua hydrogen atoms were located from Fourier difference maps and constrained with equal O-H distances. All the non-hydrogen atoms were anisotropically refined. The triflate anion in **6** crystallised with an almost 50 % positional disorder recorded.

Equilibrium Studies

The substitution of methanol in *fac*-$[Mn(CO)_3(L,L'\text{-Bid})(CH_3OH)]^n$ complexes by a range of entering ligands could be studied as *pseudo* first-order processes defined by the simple equilibrium which exists, as indicated in Eq 1,

Equation 1

$$fac\text{-}[Mn(CO)_3(L,L'\text{-Bid})(CH_3OH)]^n + X \underset{k_{-1}}{\overset{k_1, K_1}{\rightleftharpoons}} fac\text{-}[Mn(CO)_3(L,L'\text{-Bid})(X)]^n + CH_3OH$$

where n = (1 + m); m = 0, −1 = charge of chelated bidentate ligand, while the charge of the entering nucleophile X is not specified.

The stability constant (K_1) for the reaction between *fac*-$[Mn(CO)_3(L,L'\text{-Bid})(CH_3OH)]^n$ complexes and various monodentate entering ligands (X) has been determined kinetically using the definition $K_1 = k_1/k_{-1}$. It was also obtained by nonlinear least-squares analysis using the established relationship based on UV/vis data, $A_{obs} = (A_M + A_{ML}K_1[X])/(1 + K_1[X])$, as reported previously[25] with A_M and A_{ML} the absorbance of the *fac*-$[Mn(CO)_3(L,L'\text{-Bid})(CH_3OH)]^n$ and *fac*-$[Mn(CO)_3(L,L'\text{-Bid})(X)]^n$ complexes, A_{obs} the observed absorbance and [X] the concentration of the entering ligand respectively. Only one reaction was spectroscopically observed for every kinetic run performed in this study, indicating a one-step process for all the different entering nucleophiles (X) investigated.

Kinetic Data Treatment. The kinetic runs were performed under *pseudo*-first-order conditions with the entering ligand in large excess in each case. Least-squares analyses were performed on the absorbance *vs* time data obtained from the kinetic runs to appropriate functions using MicroMath Scientist.[26] The solid lines in the figures presented are computer least-squares fits of data, while the experimental values are represented as individual points. The concentration dependence of the *pseudo*-first-order rate constant (k_{obs}) for the substitution process of the methanol ligand in the *fac*-$[Mn(CO)_3(L,L'\text{-Bid})(CH_3OH)]^n$ complexes by monodentate entering ligands (indicated X) is given by Equation 2. The kinetics are monitored where [X] ≫ [Mn], with typical metal concentrations ranging from 4×10^{-5} to 1×10^{-4} M. The rates and concentration dependences obtained in this study assumes that the aqua complexes, immediately upon dissolution in methanol, exchange the coordinated aqua to form the corresponding *fac*-$[Mn(CO)_3(L,L'\text{-Bid})(CH_3OH)]^n$ complexes.

Equation 2

$$k_{obs} = k_1[X] + k_{-1}$$

Results

Synthesis and Charaterization

Special care had to be taken throughout to ensure that the complexes were not exposed to light. In terms of **1** and **6**, the bromide anions were first abstracted by using $AgCF_3SO_3$. The AgBr that formed was dried and weighed in each case to confirm quantitative replacement of Br^- from the Mn(I) synthon. The ^{1}H and ^{13}C NMR, together with the other presented data, support the synthetic results. The substitution products were also obtained and fully characterized.

The X-ray crystal structures for **1** and **6** were determined and crystallographic data, selected bond angles and bond lengths are reported in Tables 1 and 2. The complex structures of **1** and **6** are shown in Figure 1a and 1b, respectively, with their corresponding atom numbering schemes.

Table 1. Crystallographic data of *fac*-$[Mn(CO)_3(Bipy)(H_2O)][CF_3SO_3]$ (**1**) and *fac*-$[Mn(CO)_3(Phen)(H_2O)][CF_3SO_3]$ (**6**).

Crystallographic Data	**1**	**6**
Empirical Formula	$MnC_{14}H_{10}F_3N_2O_7S$	$MnC_{16}H_{10}F_3N_2O_7S$
F.W.	462.25	486.27
Crystal System	Monoclinic	Monoclinic
Space Group	$P2_1/n$	$P2_1/n$
a (Å)	10.6620(4)	10.220(1)
b (Å)	9.6493(4)	10.514(1)
c (Å)	17.1370(7)	17.379(2)
α (°)	90	90
β (°)	93.195(2)	90.604(5)
γ (°)	90	90
Volume (A^3)	1760.3(2)	1867.3(3)
Z	4	4
ρ_{calc} ($g.cm^{-3}$)	1.744	1.730
Crystal colour	Yellow	Yellow
Crystal morphology	Cuboid	Needle
Crystal size (mm)	0.365 × 0.228 × 0.211	0.39×0.089×0.069
μ (mm^{-1})	0.941	0.892
F (000)	928.0	976.0
θ range (°)	2.20 - 28.39	2.26 - 28.37
Index ranges	$-14 \le h \le 14$ $-12 \le k \le 12$ $-21 < l < 22$	$-13 \le h \le 13$ $-13 \le k \le 14$ $-23 < l < 23$
Reflections collected	24272	32050
Unique reflections	4410	4648
Reflections with $I > 2\sigma(I)$	3744	3477
R_{int}	0.0479	0.0458
Completeness to 2 theta (°, %)	28.39, 99.7	28.37, 99.1
Data/ restraints/ parameters	4410 / 22 / 315	4648 / 3 / 279
GooF	1.042	1.025
R [$I > 2\sigma(I)$]	$R_1 = 0.0446$ $wR_2 = 0.1000$	$R_1 = 0.0401$ $wR_2 = 0.0943$
R (all data)	$R_1 = 0.0536$ $wR_2 = 0.1068$	$R_1 = 0.0599$ $wR_2 = 0.1038$
ρ_{max}, ρ_{min} ($e\ A^{-3}$)	1.054, -1.081	0.556, -0.588

Table 2. Selected bond distances (Å) and angles (°) for **1** and **6**.

Bond distance	**1**	**6**
Mn01 - C01	1.795(3)	1.801(3)
Mn01 - C02	1.806(3)	1.811(2)
Mn01 - C03	1.812(3)	1.823(3)
Mn01 - N02	2.041(2)	2.058(2)
Mn01 - N01	2.042(2)	2.051(2)
Mn01 - O04	2.068(2)	2.073(2)
Bond angle	**1**	**6**
C01 - Mn01 - C02	86.96(13)	87.42(11)
C01 - Mn01 - C03	90.42(12)	91.32(11)
C02 - Mn01 - C03	86.78(13)	87.52(11)
C01 - Mn01 - N02	91.86(10)	92.49(10)
C01 - Mn01 - N01	94.87(11)	91.90(10)
N02 - Mn01 - N01	79.31(8)	80.33(8)
C01 - Mn01 - O04	174.75(10)	174.50(9)
C02 - Mn01 - N02	174.74(10)	176.04(9)
C03 - Mn01 - N01	174.28(10)	175.53(9)

All the respective products from ligand substitution reactions of the coordinated methanol in the *fac*-$[Mn(CO)_3(L,L'\text{-Bid})(CH_3OH)]^n$ complexes were also characterized *in situ* by UV/vis and were successfully compared to the data obtained from the syntheses. The rates and concentration dependences obtained in this study assume that the aqua complexes exchange the coordinated aqua ligand for a methanol ligand to form the corresponding solvated *fac*-$[Mn(CO)_3(L,L'\text{-Bid})(CH_3OH)]^n$ complexes, as soon as the complex is dissolved in methanol. The products were also confirmed by the kinetic runs, where simple first-order substitution processes were observed for all the reactions studied and only one product is clearly formed, also indicated by the formation of isosbestic points for all the reactions studied, see Figure 4.

Further confirmation of the immediate formation of *fac*-$[Mn(CO)_3(L,L'\text{-Bid})(CH_3OH)]^n$ upon dissolution of the corresponding aqua complexes in methanol is provided by the successful isolation and characterization of complexes wherein methanol is coordinated in the (previous) aqua site, as manifested by **2**, **7**, **12** and **17**. The stability constants have been calculated as described above and is reported with the rate constants and activation parameters, in Table 3. Figure 2 illustrates the data treatment to determine the stability constants (K_1) spectrophotometrically.

Journal Name RSCPublishing

ARTICLE

Figure 1. Molecular diagram with numbering scheme of (a) *fac*-[$Mn(CO)_3(Bipy)(H_2O)$][CF_3SO_3] (**1**) and (b) *fac*-[$Mn(CO)_3(Phen)(H_2O)$][CF_3SO_3] (**6**). The anions and hydrogen atoms are omitted for clarity.

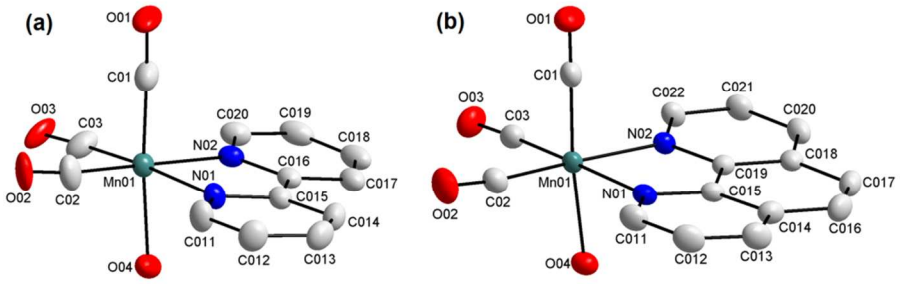

Table 3. Rate constants, equilibrium constants and activation parameters for the reactions between *fac*-[$Mn(CO)_3(Bipy)(CH_3OH)$][CF_3SO_3] (**2**), *fac*-[$Mn(CO)_3(Phen)(CH_3OH)$][CF_3SO_3] (**7**), *fac*-[$Mn(CO)_3(Pico)(CH_3OH)$] (**12**) and *fac*-[$Mn(CO)_3(2,4\text{-}QuinH)(CH_3OH)$] (**17**) and entering monodentate ligands in methanol, 25.0 °C.

	2	**7**	**12**	**17**
		Bromide ions (Br^-)		
k_1 ($M^{-1}s^{-1}$)	3.1(1) x 10^{-1}	5.0(2) x 10^{-1}	4.7(4) x 10^{-1}	
k_{-1} (s^{-1})	9.7(6)x10^{-3}	2.2(1) x 10^{-2}	2.0(2) x 10^{-2}	
K_1 (M^{-1})	32±2	23±1	24±3	
K_1 [a] (M^{-1})	24±6	24±7	45±8	
$\Delta H^{\neq}_{k1}$ (kJ mol^{-1})		66.7±0.6	68±2	
		63±3[b]	63±4[b]	
$\Delta S^{\neq}_{k1}$ (J K^{-1} mol^{-1})		-27±2	-24±5	
		-40±9[b]	-39±12[b]	
		Pyridine (Py)		
k_1 ($M^{-1}s^{-1}$)	2.93(9) x 10^{-3}	2.39(5) x 10^{-3}	9.4(1) x 10^{-1}	4.5±0.2
k_{-1} (s^{-1})	9(5) x 10^{-4}	1.5(3) x 10^{-5}	1.3(7) x 10^{-4}	4(1) x 10^{-2}
K_1 (M^{-1})	3±2	159±32	7231±3894	113±29
K_1[a] (M^{-1})	21±5	65±19	86±25	47±16
$\Delta H^{\neq}_{k1}$ (kJ mol^{-1})		80±3	61±1	
		85±3[b]	56±9[b]	
$\Delta S^{\neq}_{k1}$ (J K^{-1} mol^{-1})		-25±11	-42±4	
		-12±10[b]	-56±27[b]	
		Thiourea (TU)		
k_1 ($M^{-1}s^{-1}$)	9.53(3) x 10^{-2}	7.4(2) x 10^{-2}	4.31±0.02	7.6±0.7
k_{-1} (s^{-1})	3.6(2) x 10^{-4}	2.3(1) x 10^{-3}	2.5(1) x 10^{-2}	3.1(5) x 10^{-1}
K_1 (M^{-1})	265±15	32±2	172±7	24.5±0.5
K_1[a] (M^{-1})	104±23	203±88	104±19	84±23
$\Delta H^{\neq}_{k1}$ (kJ mol^{-1})		57±5	54±2	
		50±3[b]	53±2[b]	
$\Delta S^{\neq}_{k1}$ (J K^{-1} mol^{-1})		-77±15	-51±6	
		-100±10[b]	-55±6[b]	

[a] = Spectrophotometrically determined from A_{obs} *vs* [ligand] data. [b] = Obtained from global fits of [L], temperature and k_{obs} values.

Journal Name RSCPublishing

ARTICLE

Kinetics of Coordinated Methanol Substitution. The substitution kinetics of coordinated methanol in *fac*-$[Mn(CO)_3(L,L'\text{-Bid})(CH_3OH)]^n$ type complexes by various entering ligands was studied as simple first-order processes defined by the single equilibrium described in Equation 1. Previous studies indicated that the substitution of the water ligands in the tri aqua species, *fac*-$[M(CO)_3(H_2O)_3]^+$ (M= Mn, Tc, Re) by different ligands, proceeded in three simple steps to yield predominantly mono-, di, or trisubstituted products.5[27,28] In the current study, the monosubstitution products were confirmed by chemical and spectroscopic analysis. Similar procedures were followed and results obtained for the substitution of coordinated methanol in the rhenium analogue, *fac*-$[Re(CO)_3(L,L'\text{-Bid})(CH_3OH)]^n$. Solutions of *fac*-$[Mn(CO)_3(L,L'\text{-Bid})(CH_3OH)]^n$ and different entering ligands were evaluated by NMR and IR spectroscopy and no tendency of bidentate ligand dissociation could be observed, nor changes in the absorbance spectra, thus indicating that the one reaction observed in each case is indeed methanol substitution. All of the complexes used in this study are very insoluble in water and for this reason methanol was used as solvent. The stability of all the complexes in methanol was established by monitoring the solutions on a UV/vis spectrophotometer for 72 hours. The second order rate constants as observed, clearly indicate that even the least reactive complexes completely solvate to the corresponding methanol species within a few hours, with most requiring only minutes or even seconds. This was confirmed by monitoring the kinetics on freshly prepared solutions, allowing these to stand for different appropriate times, ranging from minutes to hours, and re-monitoring the reactions. No change in the rates of the reactions or deviations from first order kinetics could be observed, leading to the conclusion that the complexes were completely solvated upon commencement of the kinetic runs to study the substitution processes.

Figure 3. (a) A typical UV/vis spectral change for the methanol substitution reaction between *fac*-$[Mn(CO)_3(Bipy)(CH_3OH)]^+$ (5 x 10^{-4} M) and pyridine (0.2 M) in methanol at 25.0 °C and (b) a fit of absorbance *vs* time data for this reaction at 370 nm, Δt = 840 sec, t_{tot} = 8 400 s.

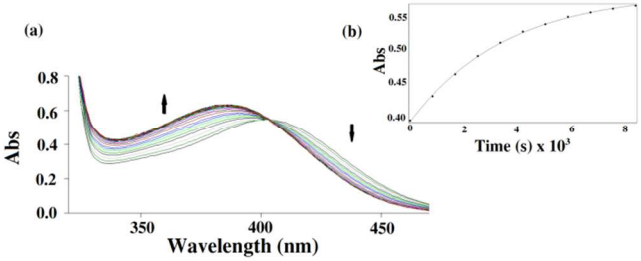

The methanol substitution in complexes **2**, **7**, **12** and **17** was analyzed for a range of monodentate entering ligands. The time-resolved absorbance change values (Figure 3) were then fitted to single exponentials (line in Figure 3 (b)) confirming first-order behaviour. All plots of k_{obs} *vs* ligand concentrations yielded straight lines and the data was fitted to Equation 2 using linear least-squares analysis.[26]

Figure 4. Selected plots of ligand concentration *vs* k_{obs} values obtained for (a) *fac*-$[Mn(CO)_3(Bipy)(CH_3OH)]^+$, [Mn] = 5.0 x 10^{-4} M, (b) *fac*-$[Mn(CO)_3(Phen)(CH_3OH)]^+$, [Mn] = 5.0 x 10^{-4} M, (c) *fac*-$[Mn(CO)_3(Pico)(CH_3OH)]$, [Mn] = 3.0 x 10^{-3} M and (d) *fac*-$[Mn(CO)_3(2,4\text{-QuinH})(CH_3OH)]$, [Mn] = 2.0 x 10^{-4} M in methanol at 25.0 °C.

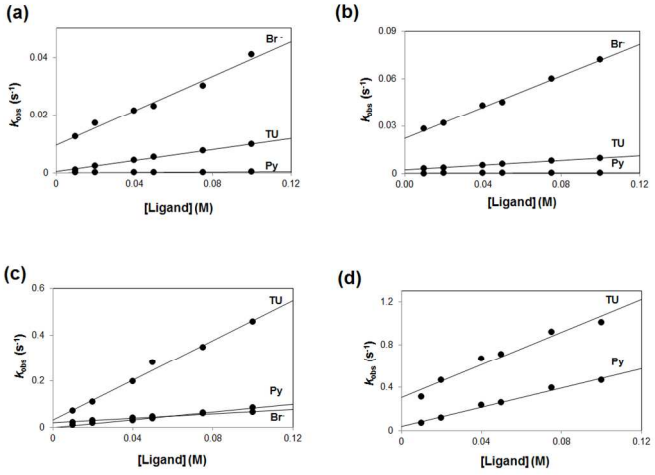

In Figure 4 (a) – (d) a summary of some of the reaction plots for **2**, **7**, **12**, and **17** with different entering ligands are illustrated. The rate and equilibrium constants together with the activation parameters obtained from Eyring plots are reported in Table 3. The results obtained for the methanol substitution reactions for *fac*-$[Mn(Bipy)(CO)_3(CH_3OH)]^+$, *fac*-$[Mn(Phen)(CO)_3(CH_3OH)]^+$, *fac*-$[Mn(Pico)(CO)_3(CH_3OH)]$ and *fac*-$[Mn(2,4\text{-QuinH})(CO)_3(CH_3OH)]$ with different entering ligands (Br^- ions, pyridine and thiourea) are systematically reported here. Selective data for systems as indicated in Table 3 have also been analyzed with a global fit utilizing all the individual k_{obs} *versus* [L] *versus* temperature data points. It is clear that the traditional Eyring plots yielded similar results and do not influence conclusions made.

N,N'-Bidentate Ligands. (*fac*-$[Mn(Bipy)(CO)_3(CH_3OH)]^+$ and *fac*-$[Mn(Phen)(CO)_3(CH_3OH)]^+$). The rates of coordinated methanol substitution in *fac*-$[Mn(CO)_3(Bipy)(CH_3OH)]^+$ with pyridine, thiourea and Br^- ions were monitored at 25.0 °C by UV/vis spectroscopy at 370 nm, 365 nm and 445 nm respectively. The reactions between *fac*-$[Mn(Phen)(CO)_3(CH_3OH)]^+$ and pyridine,

thiourea and Br^- ions were performed at 15.0 °C, 25.0 °C, 35.0 °C and 45.0 °C. These reactions were followed at the following wavelengths: 370 nm for the reaction with pyridine, 375 nm for the reaction with thiourea and 370 nm for the Br^- ions. The rate and equilibrium data are given in Table 3 and the data fits are illustrated in Figure 4 (a) and (b). **N,O-Bidentate Ligands. (***fac*-[Mn(Pico)$(CO)_3(CH_3OH)$] and *fac*-[Mn(2,4-QuinH)$(CO)_3(CH_3OH)$]). The methanol substitution reactions of *fac*-[Mn$(CO)_3$(Pico)(CH_3OH)] by pyridine, thiourea and bromide ions were monitored at four different temperatures (15.0 °C, 25.0 °C, 35.0 °C and 45.0 °C) by UV/vis spectroscopy at 365 nm, 385 nm and 415 nm respectively. For *fac*-[Mn$(CO)_3$(2,4-QuinH)(CH_3OH)], the reactions at 25. 0 °C with pyridine and thiourea were too fast for normal UV/vis spectrophotometry and were followed on a stopped-flow system at 380 nm and 395 nm respectively. Unfortunately, the data obtained for the bromide ions as entering ligands did not provide good least-square non-linear fits of A_{obs} *vs* time data, possibly partly due to the poor solubility of the metal complexes and was therefore not included. The rate and equilibrium data for the N,O bidentate ligands is also given in Table 3 with representative fits illustrated in Figure 4 (c) and (d).

Discussion

Synthesis. All care has been taken to perform the syntheses in the absence of light because of the sensitivity of Mn(I) to light. In most cases high yields were obtained similar to previous publications.[34] The low yields obtained for the aqua complexes cannot be explained off hand but a search of the CSD indicates there are only two related complexes where suitable crystals for X-ray diffraction were obtained, suggesting that these complexes might be difficult to obtain in high yields. In the cases where the coordinated water was replaced by other monodentate ligands, higher yields were obtained.

X-ray Crystallography. Both **1** and **6** crystallize in the monoclinic space group, $P2_1/n$. The asymmetric units in both crystals consist of the parent molecular compound and one $CF_3SO_3^-$ counter ion. In general for both the structures presented here, the coordination geometry around the Mn(I) center is a distorted octahedron consisting of three facially coordinated CO ligands, a bidentate ligand and a coordinated water molecule.

The Mn-N bond distances [(**1**) 2.041(2) and 2.042(2) Å; (**6**) 2.058(2) and 2.051(2) Å] compare well with other Mn(I) structures in literature.[29,30,31,32] It is also similar to the distances observed in some Re(I) structures with Re-N distances ranging from 2.168(4) Å to 2.178(8) Å,[15,33] the relative increase in bond lengths being typical when descending in a triad from a 3d to a 5d metal centre. The N01-Mn-N02 bite angles of 79.31(8) ° and 80.33(8) ° for **1** and **6** respectively, are also consistent with other similar structures and are probably the reason for the slight distortion of the coordination polyhedra in both cases. The Mn-O04 bonding distances are reported as 2.068(2) and 2.073(2) Å for **1** and **6** and also compares well with other aqua complexes with distances of 2.108(5) Å[32] and 2.099 Å.[31]

Both structures exhibit extensive hydrogen bonding networks (see Supporting Information) with the counter ions serving as links between the metal compounds. π-Stacking interactions with centroid to centroid distances of 3.6928(1) Å and 4.0856(1) Å for **1** and 3.9034(3) Å for **6** further support the intricate stability of the crystal lattice.

The triflate anion in **1** displays positional disorder over two positions in a 0.4 : 0.6 ratio.

UV/vis and IR Spectroscopy. The UV/vis data is typical for Mn(I) tricarbonyl complexes and once ligand substitution have been affected, typical UV/vis transitions are observed.[34,35,36] The effect of variation from *N,N*' to *N,O*' bidentate ligands is not as pronounced (as observed in molar extinction coefficients) as was observed for the Re(I) counterparts, as expected.[15] In terms of IR, no clear tendencies in either symmetric or asymmetric stretching frequencies were observed other than what was reported before.[34]

Stability Constants. The stability constants, K_1, for the ligation reaction in Equation 1 are listed in Table 3, and there is a reasonable to good agreement of the kinetically *vs* thermodynamically determined values. In general, the indication is that there is an under estimation in the k_{-1} values, as illustrated by the slightly lower values obtained for the thermodynamically determined K_1 in most cases. This would indicate an over-estimation of the kinetically determined stability constants. Nevertheless, there is a progressive change in the stability constants, K_1, of all the *fac*-[Mn$(CO)_3$(*L,L'*-Bid)(X)]^n complexes as follows: TU > Br^- ~ Py. This could possibly be due to the softness of the S-donor ligand and was also found in the formation studies of *fac*-$[Mn(CO)_3(H_2O)_2(L)]^+$ (L = DMS, CH_3CN), where K_1(DMS) was almost one order of magnitude larger than $K_1(CH_3CN)$.[37]

Substitution Kinetics.

N,N'-Bid Ligands (*fac*-$[Mn(CO)_3(Bipy)(CH_3OH)]^+$ (**2**) and *fac*-$[Mn(CO)_3(Phen)(CH_3OH)]^+$ (**7**)). From Table 3 it can be seen that the rates of formation, k_1, for Br^-, Py and TU as entering ligands are comparable for **2** and **7** and that $k_1(Br^-)$ [**2**: 0.31±0.01; **7**: 0.50±0.02] > k_1(TU) [**2**: 9.53(3) x 10^{-2}; **7**: 7.4(2) x 10^{-2}] > k_1(Py) [**2**: 2.93(9) x 10^{-3}; **7**: 2.39(5) x 10^{-3}]. In general, $k_1(Br^-)$ [**2**: 0.31±0.01; **7**: 0.50±0.02] is two orders of magnitude faster than k_1(Py) [**2**: 2.93(9) x 10^{-3}; **7**: 2.39(5) x 10^{-3}] for both complexes and respectively three and six times faster than k_1(TU) for both **2** and **7** [**2**: 9.53(3) x 10^{-2}; **7**: 7.4(2) x 10^{-2}]. On first observation this would indicate an associatively activated process, but the values for the reverse reactions, k_{-1}, also show a variation of only two orders of magnitude. This was not observed for the substitution reactions of the similar rhenium (I) complexes[15] where the forward rate constants varied much more than the reverse rates upon using different entering ligands. Grundler *et al.* investigated the complex formation of *fac*-$[Mn(CO)_3(H_2O)_3]^+$ by ^{17}O NMR and by using dimethyl sulfide (DMS) and acetonitrile (CH_3CN) as entering ligands.[13] Values of 1.75 and 5.34 M^{-1} s^{-1} for k_1 were obtained for the formation of *fac*-$[Mn(CO)_3(H_2O)_2(L)]^+$ (L = DMS, CH_3CN) for CH_3CN and DMS respectively. Their high pressure studies indicated an I_d mechanism for these substitution processes as opposed to the mechanistic changeover from I_a to I_d observed for similar reactions with Re(I) tricarbonyls.

A comparison between the reactions for *fac*-[M$(CO)_3$(N,N'-Bid)$(CH_3OH)]^n$ (M = Mn, Re) with Br^-, and Py indicates that the reactions with M = Re(I) are in general 1 order of magnitude slower than similar reactions for M = Mn(I) for the reactions with N,N'-Bid

= Bipy/Phen. This is consistent with what was expected since previous work found that a two order-of-magnitude increase in the sequence, Mn > Tc > Re, was observed for the second order rate constant for the substitution of the first aqua ligand in the triaqua *fac*-$[M(CO)_3(H_2O)_3]^+$ complexes (M = Mn, Tc and Re).[13] One would expect the first substitution step to be much faster than the following steps and as a result one would also expect to observe a smaller increase in rate when looking at the substitution of the last ligand.

N,O-Bid Ligands (*fac*-$[Mn(CO)_3(Pico)(CH_3OH)]$ (**12**) and *fac*-$[Mn(CO)_3(2,4\text{-}QuinH)(CH_3OH)]$ (**17**)). Unfortunately, reliable data for the reactions of (**17**) with Br^- ions could not be obtained under our reaction conditions, possibly due to low solubility. Nevertheless, all in all the data in Table 3 provides very interesting results. It is clear from this table that k_1 for Br^- [0.47±0.04] as entering ligand is only about 2 times slower than k_1(Py) [0.94±0.04] for the reactions of *fac*-$[Mn(CO)_3(Pico)(CH_3OH)]$ but that the corresponding reaction with TU exhibits a forward rate constant of 4.31±0.02 M^{-1} s^{-1}, virtually 10 times faster than $k_1(Br^-)$. This results in a trend k_1(TU) > k_1(Py) > $k_1(Br^-)$ for **12**, which is repeated for (and comparable to) **17** [k_1 (Py) = 4.5±0.2; k_1 (TU) = 7.6±0.7], excluding the data for Br^- as mentioned, and opposite to what was found for reactions where the N,N'-Bid ligands were coordinated to Mn(I). The reason for this is possibly that the metal complexes are positively charged when coordinated to N,N'-Bid ligands, as opposed to the neutral complexes that are attained when N,O-Bid ligands are used. On face value then, the higher affinity of a positively charged metal complex for a negatively charged halide ligand indicates an I_d mechanism.

More interesting observations can be made from the comparison of forward rate constants, k_1, for the positively charged **2** and **7** to that of **12** and **17** (neutral complexes). For the reactions with Br^-, k_1 for **2** and **7** are comparable to the value of 0.47(4) M^{-1} s^{-1} found for **12**. This was also found for the similar study on Re(I) tricarbonyls.[15] This observation is significantly reversed when the rate constants of **2** and **7** are compared to those of **12** and **17** for the reactions with Py and TU. The largest increases in k_1 for Py and TU respectively is observed when comparing k_1 of **7** (Py: 2.39(5) x 10^{-3}; TU: 7.4(2) x 10^{-2}] to that of **17** [Py: 4.5±0.2; TU: 7.6±0.7] for both entering ligands, with an almost 2000 times higher activation achieved for **17** in the case of Py and 1000 times in the case of TU. Once again this was also found for the similar study with rhenium(I) with Py as entering ligand (TU was not used in the rhenium study). These results however, point towards an I_d mechanism for the neutral complexes since one would expect the positively charged complexes to be more reactive towards substitution in purely associatively activated processes.

A comparison of the forward rates of substitution for the reactions of **12** and **17** with Py [**12**: 0.94±0.01; **17**: 4.5±0.2] to that of the similar reactions obtained previously for rhenium[15] indicates that these are between 500 and almost 1500 times faster [**Re-Pico**: 1.6(1) x 10^{-3}; **Re-2,4-QuinH**: 3.31(2) x 10^{-3}]. The same is not observed when comparing k_1 for the Br^- reactions. Here an increase in reactivity of about 1 order-of-magnitude is achieved when moving from Re(I) [**Re-Pico**: 1.18(1) x 10^{-2}] to Mn(I) [**12**: 0.47±0.04]. The effect of the bidentate ligand on the substitution processes is also evident, given the data above. It is clear from this that the N,O ligands are able to activate these reactions approximately 3 orders-of-magnitude (e.g. considering k_1(TU) for **2** *vs* **17**) more than its N,N' counterparts. This increase cannot only be ascribed to the difference in charge of the metal complexes depending on the type of bidentate ligand used, since a similar study on rhenium found an increase of > 4 order-of-magnitude when comparing N,N', to N, O and O,O' bidentate ligands.

The increased rates of substitution for Mn(I) complexes compared to Re(I), was also observed by others.[37] The fact that the general difference between k_1(Mn) *vs* k_1(Re) for the substitution reactions of *fac*-$[M(CO)_3(N,N'\text{-}Bid)(CH_3OH)]^n$ (M = Mn, Re) with various entering ligands is not as pronounced as the data found for the substitution of the first aqua ligand in *fac*-$[M(CO)_3(H_2O)_3]^+$ (M = Mn, Re, Tc) is not clear with the current data available, but it is possibly related to the fact that the substitution process of the third aqua ligand (or CH_3OH in our case) proceeds slower than those of the second and third respectively, giving rise to the possibility of an 'evening out' of the rate of the third substitution processes. Since no data is available for the substitution processes of the third aqua ligand in *fac*-$[M(CO)_3(H_2O)_3]^+$, further consideration of this should be left until proper comparisons can be made.

Another interesting observation is made when comparing the forward rate constants, k_1, for the reactions with TU in this study and the formation reaction of *fac*-$[Mn(CO)_3(H_2O)_2(DMS)]^+$, since both are sulphur donating ligands. Grundler *et al.* reported k_1(DMS) as 5(2) M^{-1} s^{-1}.[13] This is about 50 times faster than what was found for **2** and **7** and in the same order than that found for **12** and **17**. This is an indication of the increasing ability of N,N'-Bid to N,O-Bid type ligands to activate the manganese (I) tricarbonyl center towards substitution and is similar to what was observed for the comparative studies on rhenium.

In summary, the following can be highlighted: The coordinated methanol substitution reactions from the Mn(I) complexes **2**, **7**, **12** and **17** by various entering nucleophiles were investigated. From this data it was observed that the first-order rate constants, k_1, decrease in general for Br^- > TU > Py for the positively charged **2** and **7.** This decrease is generally consistent with the nucleophilicity of the entering ligands as illustrated by its pK_a values and supports an associative activated type mechanism for these reactions. The order of decrease for **12** and **17** is switched around in the order TU > Br^-~ Py and is attributed to the softness of TU and the different charge (as opposed to **2** and **7**) of these complexes.

Activation Parameters. The activation parameters in Table 3 together with the kinetic data indicate that the substitution process of the *fac*-$[Mn(CO)_3(L,L'\text{-}Bid)(CH_3OH)]^n$ complexes most likely proceed *via* an interchange mechanism, with the cationic Bipy **2** and Phen **7** complexes leaning toward I_a, while the neutral complexes of N,O-Bid (**12** and **17**) might suggest an I_d mechanism. If the I_d character as determined by Grundler *et al.* for the formation of *fac*-$[Mn(CO)_3(H_2O)_2(L)]^+$ type complexes is considered, as opposed to the change over from I_a to I_d for the similar rhenium complexes depending on entering ligands used, it would be safe to suggest an I_d mechanism here. However, more information, including high-pressure studies would cast more light on this aspect of the investigation.

Conclusion

The effects of different bidentate donor ligands on the reactivity of the Mn(I) metal center were illustrated by the use of N,N′- and N,O-Bid ligands. A general trend of k_1 for the Mn(I) complexes defined in **17** > **12** > **7** > **2** was observed. Grundler and co-workers obtained a value of 5(2) M^{-1} s^{-1} for the formation of *fac*-$[Mn(CO)_3(H_2O)_2(DMS)]^+$. This is about 50 times faster than what was found for **2** and **7** and in the same order of magnitude than that found for **12** and **17**. This is an indication of the increasing ability when moving from the N,N'-Bid to N,O-Bid type ligands to activate the manganese (I) tricarbonyl center towards substitution and is similar to what was observed for the comparative studies of rhenium (I).

It was concluded that the N,O-Bid type donor ligands utilized here activate the metal center substantially more than the N,N'-Bid type ones and that positively charged complexes have slower coordinated methanol substitution rates in general. More data and a wider range of complexes may have to be investigated in future studies to gain a better understanding of the intimate mechanism of these reactions.

The greater significance of our results is that this is the first study of its kind on Mn(I) tricarbonyl complexes and it indicates that Mn(I) complexes can be used as models to study the more relevant Tc (I) chemistry (to radiopharmacy). Furthermore, it shows how reactivity can be tuned by simple variation of the bidentate ligand, following the [2 + 1] approach and links onto the previous work done on rhenium (I) where 4 orders of magnitude activations were achieved.

In general, the mechanism of octahedral substitution reactions tend to be dissociative of nature (D or I_d). Our results, while not conclusive, also suggest an I_d mechanism for all the reactions studied (negative values for $\Delta S^{\neq}$). In terms of radiopharmaceutical design this is a positive result since the rate of the formation of a potential drug is not dependant on the entering group which means that a great variation of entering groups could be utilized without influencing the time of synthesis.

Acknowledgements

Financial assistance from the University of the Free State is gratefully acknowledged. We also express our gratitude towards SASOL, PETLabs Pharmaceuticals, the South African National Research Foundation (SA-NRF/THRIP) and the University of the Free State Strategic Academic Initiative (Advanced Biomolecular Systems) for financial support of this project. This work is based on the research supported in part by the National Research Foundation of South Africa (Grant specific unique reference number (UID) 84913). The Grantholder acknowledges that opinions, findings and conclusions or recommendations expressed in any publication generated by the NRF supported research are that of the authors, and that the NRF accepts no liability whatsoever in this regard.

Notes and references

Department of Chemistry, University of the Free State, P.O. Box 339, Bloemfontein 9300, South Africa. visserhg@ufs.ac.za

Supporting information. CCDC 1008981 and CCDC 1008982 contain the supplementary crystallographic data for **1** and **6**. This data can be obtained free of charge from The Cambridge Crystallographic Data Centre *via* www.ccdc.cam.ac.uk/data_request/cif.

[1] F. Zobi, O. Blacque, R.K.O. Sigel, R. Alberto, *Inorg. Chem*., 2007, **46**, 10458-10460;

[2] B. Spingler, S. Mundwiler, P. Ruiz-Sanchez, D.R. van Staveren, R. Alberto, *Eur. Jour. Inorg. Chem*., 2007, **18**, 2641-2647;

[3] B. Spingler, S. Mundwiler, P. Ruiz-Sanchez, D.R. van Staveren, R. Alberto, *Eur. Jour. Inorg. Chem*., 2007, **18**, 2641-2647;

[4] R. Alberto, R. Schibli, R. Waibel, U. Abram, A.P. Schubiger, *Coord. Chem. Rev*., 1999, **192**, 901-919;

[5] R. Alberto, W.A. Herrmann, P. Kiprof, F. Baumgärtner, *Inorg. Chem*., 1992, **31**, 895-899;

[6] R. Alberto, R. Schibli, U. Abram, A. Egli, F.F. Knapp, P.A. Schubiger, *Radiochim. Acta*., 1997, **79**, 99-103;

[7] R. Alberto, A. Egli, R. Schibli, U. Abram, T.A. Kaden, A.O. Schaffland, R. Schwarzbath, P.A. Schubiger, *Q. J. Nucl. Med*., 1998, **42** *(suppl)*, 9;

[8] P.D. Raposinho, J.D.G. Correia, S. Alves, M.F. Botelho, A.C. Santos, I. Santos, *Nucl. Med. Biol*., 2008, **35**, 91-99;

[9] R. Alberto, K. Ortner, N. Wheatley, R. Schibli, A.P. Schubiger, *J. Am. Chem. Soc*., 2001, **123**, 3135-3136;

[10] N.I. Gorshkov, R. Schibli, A.P. Schubiger, A.A. Lumpov, A.E. Miroslavov, D.N. Suglobov, *J. Organomet. Chem.,* 2004, **689**, 4757-4763;

[11] N. Agorastos, L. Borsig, A. Renard, P. Antoni, G. Viola, B. Spingler, P. Kruz, R. Alberto, *Chem. Eur. J*., 2007, **13**, 3842-3852;

[12] B. Salignac, P.V. Grundler, S. Cayemittes, U. Frey, R. Scopelliti, A. Merbach, *Inorg. Chem*., 2003, **42**, 3516-3526;

[13] P.V. Grundler, L. Helm, R. Alberto, A.E. Merbach, *Inorg. Chem*., 2006, **45**, 10378-10390;

[14] S. Mündwiler, M. Kündig, K. Ortner, R. Alberto, *Dalton Trans*., 2004, 1320;

[15] M. Schutte, G. Kemp, H.G. Visser, A. Roodt, A., *Inorg. Chem*., 2011, **50** (24), 12486-12498;

[16] M. Schutte, H.G. Visser, A. Roodt, *Inorg. Chem*., 2012, **51**, 11996-12006;

[17] A. Brink, H.G. Visser, A. Roodt, *Inorg. Chem*., 2013, **52**, 8950-8961;

[18] Cambridge Structural Database (CSD), Version 5.32, Feb 2011 update. F.H. Allen, Acta Crystallogr. 2002, **B58**, 380;

[19] *SAINT-Plus, version 6.02 (including XPREP)*; Bruker AXS, Inc.: Madison, WI, 1999;

[20] *SADABS, version 2004/1*; Bruker, AXS, Inc.: Madison, WI, 2004;

[21] A. Altomare, M.C. Burla, M. Camalli, G.L. Cascarano, C. Giacovazzo, A. Guagliardi, A.G.G. Moliterni, G. Polidori, R. Spagna, *J. Appl. Crystallogr*., 1999, **32**, 115-119;

[22] G.M. Sheldrick, *Acta Crystallogr*., 2008, **A64**, 112-122;

[23] L.J. Farrugia, *J. Appl. Crystallogr*., 1999, **32**, 837-838;

[24] K. Brandenburg, H. Putz, *DIAMOND, release 3.1b*, Crystal Impact GbR: Bonn, Germany, 2005;

[25] H.J. Van der Westhuizen, R. Meijboom, A. Roodt, M. Schutte, *Inorg. Chem*., 2010, **49**, 8599-9608;

[26] *Micromath Scientist for Windows*, version 2.01; MicroMath Inc.: St. Louis, MO, U.S.A., 1986-1995;

[27] M. Schutte, H.G. Visser, *Acta Crystallogr*., 2008, **E64**, m1226-m1227;

[28] M. Schutte, H.G. Visser, A. Roodt, *Acta Crystallogr*., 2008, **E64**, m1610-m1611;

[29] G. Ara, S.E. Kabir, K. Kundu, K.M.A. Malik, *J. Chem. Cryst*., 2003, **33**, 851-857;

[30] M.L. Valín, D. Moreiras, X. Solans, M. Font-Altaba, F.J. García-Alonso, *Acta Crystallogr*., 1986, **C42**, 417-418;

[31] E. Horn, A. Horiuchi, *Z. Kristallogr., New Cryst. Struct.,* 2001, **216**, 3074;

[32] N. Antón, M. Arroyo, P. Gómez-Iglesias, D. Miguel, F. Villafañe, *J. Organomet. Chem*., 2008, **693**, 3074-3080;

[33]G. Kemp, PhD Dissertation, University of Johannesburg, 2006;

[34] C. Pereira, H.G. Ferreira, M.S. Schultz, J. Milanez, M. Izidoro, P.C. Leme, R.H.A. Santos, M.T.P. Gambardella, E.E. Castellano, B.S. Lima-Neto, R.M. Carlos, *Inorg. Chim. Acta,* 2005, **358**, 3735-3744;

[35] M. Bakir, I. Hassan, O. Green, *J. Mol. Struct*., 2003, **657**, 75-83;

[36] C.M. Alvarez, R. García-Rodríguez, D. Miguel, D*alton Trans*., 2007, 3546-3554;

[37] H. Helm, *Coord. Chem. Rev*., 2008, **252**, 2346-2361.

Table of Contents

"Activation of the Manganese(I) Tricarbonyl Core by Selective Variation of Bidentate Ligands (*L*,*L*'-Bid = *N*,*N*'and *N*,*O* Donor Atom Sets) in *fac*-$[Mn(CO)_3(L,L'\text{-Bid})(CH_3OH)]^n$ complexes."

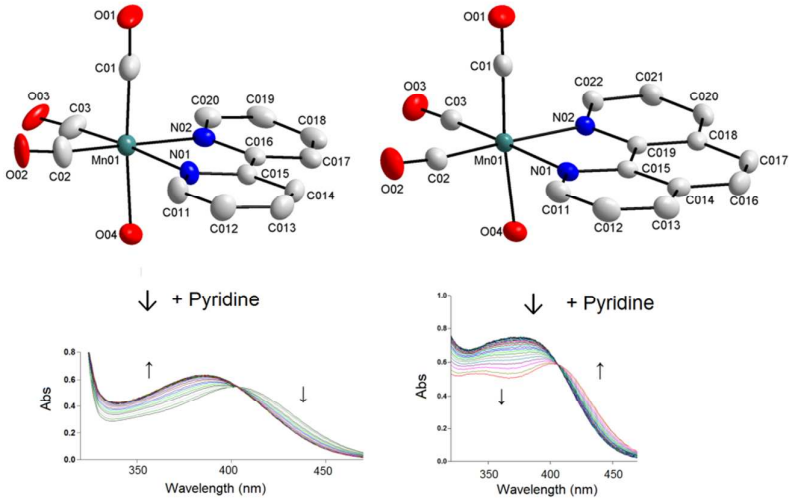

A range of *fac*-$[Mn(CO)_3(L,L'\text{-Bid})(H_2O)]^n$ complexes has been synthesized and the methanol substitution has been investigated for the first time.

Introduction	1
Experimental	2
X-ray Structure Determinations	5
Equilibrium Studies	5
Kinetic Data Treatment	5
Results	5
Synthesis and Characterization	5
Kinetics of Coordinated Methanol Substitution	8
Discussion	9
Synthesis	9
X-ray Crystallography	9
UV/vis and IR Spectroscopy	9
Stability Constants	9
Substitution Kinetics	9
Activation Parameters	10
Conclusion	11
Acknowledgements	11
References	12